

**PARTICLE FLOW AND CONTAMINATION IN SLIDER AIR BEARINGS  
FOR HARD DISK DRIVES**

Xinjiang Shen and David B. Bogy

Computer Mechanics Laboratory, Department of Mechanical Engineering

University of California at Berkeley

Berkeley, CA 94720

**ABSTRACT**

For a particle entrained in an air bearing, various forces, such as the viscous drag force, Saffmann and Magnus lift forces and gravity force, will act on it. Such particles may pass through the air bearing or impact the slider or disk and then adhere to the surface or bounce off. In this paper, particle flow in an air bearing is simulated. The contamination of particles on a slider's surface is analyzed using the assumption of perfect adhesion upon impact. The effect of particle size and density on particle paths in the air bearing is studied. The numerical results show that particles are likely to contaminate slider surfaces in the transition regions on the rails. The density of the particles and the pitch angle of the slider are also found to strongly affect the flying path of the particles, and therefore, the accumulation of the particles on slider surfaces.

**Keywords:** Air Bearing, Particle Flow, Contamination.

## **1. Introduction**

With the evolution of magnetic recording disk technology, the flying height of the sliders has decreased dramatically. Currently, the minimum flying height in some products already is as low as 10 nm. With such narrow gaps between the slider and disk surfaces, the flow of particles and their contamination on slider surfaces become a major concern. For a particle entering the air bearing, its possible effects include modulation of the flying height, abrasive wear and mechanical scratching of the magnetic disk surface, and thermally induced spikes in the read-write signal. Flash events introduced near MR transducers will modify the MR signal because of the dependence of resistance on temperature, while mechanical scratching on magnetic disk surfaces may cause permanent data loss. Those effects depend on the size and properties of the particles and their interaction with the slider and magnetic disk surfaces. Therefore, proper slider design is necessary to reduce the particles' chances of entering the air bearing, contacting the slider and disk surfaces, and contaminating the slider surfaces.

The motion of a particle entrapped in an air bearing is quite complicated due to the various forces acting on it. The forces are not only dependent on the particle's size, density and the air velocity and pressure fields in the air bearing, but also on the relative velocities between the particle and the air bearing, and the initial entry conditions. Various expressions (Chen, 1996, Liu and Jew, 1965, Saffmann, 1965) have been derived for determining the forces acting on a particle in unsteady gas flows. Previously, Zhang and Bogoy (1996, 1997) studied the magnitudes of the Magnus lift force, the Saffmann lift force, and gravity force. The Magnus lift force is caused by the spin of a particle in a fluid. If the particle's rotation speed is zero, there

is no Magnus lift force. For very small particles, the gravity force is much smaller than the drag force. For larger particles, the gravity force may not be negligible. The drag and lift forces depend on the relative velocity between the particle and the air bearing. For air-borne particles, which have very small velocities relative to the air bearing, those forces could be on the same order of magnitude. Among those forces, the drag and lift forces play an important role for large particle contamination on slider surfaces.

In this paper, we study some particle contamination issues on slider surfaces for various particles with different sizes and densities. The collisions between particles are neglected and perfect adhesion is assumed when a particle impacts a slider surface. The air bearing flow containing the particles is assumed to be laminar because the thickness of the air bearing is very small compared with the length of the slider. First we recall the equations that determine the forces and the motion of a particle in an air bearing. Then we choose a representative currently available slider design for calculation of particle motion. Results are presented showing the effects of several of the parameters on particle motion.

## 2. Particle Kinetic Equations

The governing equations for a particle moving in air can be written as

$$\frac{dx_i}{dt} = v_i \quad (1)$$

$$m \frac{dv_i}{dt} = f_i \quad (2)$$

Where  $x_i$  and  $v_i$  are components of the position and velocity vectors of the particle, respectively;  $m$  represents the mass of the particle.  $f_i$  includes the forces of drag, Saffmann lift, Magnus lift and gravity acting on the particle. The electrostatic and

molecular forces between particles and slider surfaces are not considered here. The details of the forces are thoroughly studied by Zhang and Bogoy (1997). Substituting the various force equations into the governing equations of the particle and rearranging the terms in non-dimensional form, we obtain

$$\frac{dX_p}{dT} = R_l U_p \quad (3)$$

$$\frac{dY_p}{dT} = R_l V_p \quad (4)$$

$$\frac{dZ_p}{dT} = R_h W_p \quad (5)$$

$$\frac{dU_p}{dT} = \frac{3}{4} R_h \frac{\rho_g}{\rho_p} \frac{C_d C_{wx}}{D} \bar{U} (U_g - U_p) \quad (6)$$

$$\frac{dV_p}{dT} = \frac{3}{4} R_h \frac{\rho_g}{\rho_p} \frac{C_d C_{wy}}{D} \bar{U} (V_g - V_p) \quad (7)$$

$$\begin{aligned} \frac{dW_p}{dT} = & \frac{3}{4} R_h \frac{\rho_g}{\rho_p} \frac{C_d C_{wz}}{D} \bar{U} (W_g - W_p) + \frac{27}{32} \left( \frac{1}{\varepsilon} + \frac{11}{6} l_w^* \right) R_h \text{Re}_h^{-1/2} \frac{\rho_g}{\rho_p} \frac{\hat{U}}{D} k^{1/2} \\ & + R_h \left( \frac{\rho_g}{\rho_p} - 1 \right) \frac{h_m}{\hat{U}^2} g_z + \frac{3}{4} R_h \frac{\rho_g}{\rho_p} \left( \frac{\Omega_{py}}{R_h} - 1/2 \frac{\partial U_g}{\partial z} \right) (U_g - U_p) \\ & - \frac{3}{4} R_h \frac{\rho_g}{\rho_p} \left( \frac{\Omega_{px}}{R_h} + 1/2 \frac{\partial V_g}{\partial z} \right) (V_g - V_p) \end{aligned} \quad (8)$$

$$\frac{d\Omega_{py}}{dT} = -60 \frac{R_h^2}{\text{Re}_h D^2} \frac{\rho_g}{\rho_p} \left( \frac{\Omega_{py}}{R_h} - 1/2 \frac{\partial U_g}{\partial z} \right) \quad (9)$$

$$\frac{d\Omega_{px}}{dT} = -60 \frac{R_h^2}{\text{Re}_h D^2} \frac{\rho_g}{\rho_p} \left( \frac{\Omega_{px}}{R_h} + 1/2 \frac{\partial V_g}{\partial z} \right) \quad (10)$$

where  $X = x/l$ ,  $Y = y/l$  and  $Z = z/h_m$  are non-dimensional position variables.  $l$  is the length of the slider and  $h_m$  is the initially given height of the air bearing at the

trailing edge,  $U = \frac{u}{\hat{U}}$ ,  $V = \frac{v}{\hat{U}}$  and  $W = \frac{w}{\hat{U}}$  are non-dimensional velocity components of the particle.  $T$  is the dimensionless time  $T = \hat{\Omega}t$ , and  $\hat{\Omega}$  is the rotation speed of the disk.  $\bar{U} = \sqrt{(U_g - U_p)^2 + (V_g - V_p)^2 + (W_g - W_p)^2}$ , and  $\hat{U} = \Delta U / \hat{U}$ , where  $\Delta U$  is the velocity of the sphere relative to the air flow, and  $\hat{U}$  is the disk velocity.  $U_g, V_g$  and  $U_p, V_p$  denote the velocity components in the x and y directions of the air and the sphere, respectively.  $D$  is the non-dimensional diameter of the particle, which is  $D = d / h_m$ .  $R_l$  and  $R_h$  are non-dimensional numbers, defined as  $R_l = \frac{\hat{U}}{\hat{\Omega}l}$ ,  $R_h = \frac{\hat{U}}{\hat{\Omega}h_m}$ . In Eqs. (9) and (10),  $Re_h = \frac{\hat{U}h_m}{\nu}$  is the Reynolds number,  $\Omega_{px} = \frac{\omega_{px}}{\hat{\Omega}}$ , and  $\Omega_{py} = \frac{\omega_{py}}{\hat{\Omega}}$  where  $\omega_{px}$ ,  $\omega_{py}$  are the angular velocities of the sphere with respect to x and y axis.

In order to determine the particle flow in the air bearing we need to know the gap between the slider and disk surface as well as the pressure and velocity fields in the air bearing. Since the depth of the recessed region is much smaller than its length, the airflow can be regarded as laminar. For different slip boundary conditions required by rarefaction effects at low Knudsen numbers, the momentum equations of the air film have different solutions. For the first order slip condition (Burgdorder, 1959, Lu, S and Bogy, D. B, 1994), we have

$$u_g \Big|_{z=0} = U + \lambda \frac{\partial u_g}{\partial z} \Big|_{z=0} \quad (11)$$

$$u_g \Big|_{z=h} = -\lambda \frac{\partial u_g}{\partial z} \Big|_{z=h} \quad (12)$$

$$v_g = V + \lambda \frac{\partial v_g}{\partial z} \Big|_{z=0} \quad (13)$$

$$v_g \Big|_{z=h} = -\lambda \frac{\partial v_g}{\partial z} \Big|_{z=h} \quad (14)$$

where  $h$  is the local height of the air bearing ;  $U, V$  are the speed of the disk in the  $x$  and  $y$  directions, and  $\lambda$  is the mean free path of the air. With these boundary conditions, the velocity components of the air, in non-dimensional form, are

$$U_g = \frac{P_0}{2\rho_g U^2} \frac{h_m}{l} \text{Re}_h \frac{\partial P}{\partial X} (Z^2 - ZH - Kn_h H) + \left(1 - \frac{Kn_h + Z}{2Kn_h + H}\right) \quad (15)$$

$$V_g = \frac{P_0}{2\rho_g U^2} \frac{h_m}{l} \text{Re}_h \frac{\partial P}{\partial Y} (Z^2 - ZH - Kn_h H) + \frac{V}{U} \left(1 - \frac{Kn_h + Z}{2Kn_h + H}\right) \quad (16)$$

where  $P$  is the dimensionless pressure, or pressure divided by the ambient pressure  $P_0$ ;

$H = \frac{h}{h_m}$  is a non-dimensional spacing of the air bearing;  $Kn_h = \frac{\lambda}{h_m}$  is the Knudsen

number related to the height  $h_m$ , where  $\lambda$  is the mean free path of the air molecules.

The pressure field of the air bearing,  $P$ , can be obtained from the Reynolds equation

$$\sigma \frac{\partial PH}{\partial T} = \frac{\partial}{\partial X} \left( QPH^3 \frac{\partial P}{\partial X} - \Lambda_x PH \right) + \frac{\partial}{\partial Y} \left( QPH^3 \frac{\partial P}{\partial Y} - \Lambda_y PH \right), \quad (17)$$

where  $\sigma = \frac{12\mu_g \hat{\Omega} l^2}{p_0 h_m^2}$  is the squeeze number;  $Q = 1 + 6a \frac{Kn_h}{PH}$  is the flow factor for the

first order slip model;  $a = \frac{2-\alpha}{\alpha}$  and  $\alpha$  is the accommodation factor;  $\Lambda_x$  and  $\Lambda_y$  are

the bearing numbers  $\Lambda_x = \frac{6\mu_g Ul}{p_0 h_m^2}$  and  $\Lambda_y = \frac{6\mu_g Vl}{p_0 h_m^2}$ .

For multi particle flow analysis, the number of particles and their sizes can be specified from experiments. The particles are first assumed randomly distributed outside the slider's air bearing with velocities close to the air bearing's velocity where the particles are located, which are calculated by Eqs. (15) and (16).

### 3. Numerical results and discussions

In this section, the characteristics of particle flow in a particular slider air bearing are studied. The slider, whose air bearing surface is as illustrated in Fig. 1, has a flying height of 25.6 nm; and it has a pitch angle of 75.7  $\mu$ rad and a roll of -1.79  $\mu$ rad at the radius of 14.5mm. The pressure profile is obtained by solving the Reynolds equation for the air bearing of the slider using the CML code Quick 4, and it is shown in Fig. 2. To study the particle flow in the air bearing, we first calculated the gap between the slider and the disk. The spacing results are shown in gray scale in Fig. 3 where it can be observed that particles may enter the recessed region of the air bearing through the leading rail. And particles are likely to hit the trailing rails since the gap between the trailing rails and the disk surface is much smaller than that in the recessed region. The various forces acting on a particle in the air bearing, as well as the effects of particle size and density on its flying path will be examined next. Finally, multiple particles are considered, whose sizes follow a Gaussian distribution. The particle contamination on the slider surfaces is determined by using a perfect adherence assumption on impact. The effects of particle density and slider designs on particle contamination on slider surfaces are studied to achieve better slider designs.

#### 3.1 Effects of particle sizes and densities

Particles larger than the gap between the leading rail and the disk surface will be blocked. Therefore, the particles entering the recessed region for this slider are relatively small compared with the particle size used by Zhang and Bogoy (1996, 1997). The sizes of the particles chosen here are 45, 65, 85nm. Figure 4 shows the effect of particle size on its x-z trajectory in the air bearing of the slider for the initial y-coordinate of  $y=0.2$ mm. Because the lift forces acting on a larger particle are greater than on a smaller particle, the larger particle is lifted more. Therefore, a larger particle

is more likely to contaminate the slider rail surfaces, as shown in Zhang and Bogoy (1996, 1997).

To study the material property effect on a particle's flying path in the air bearing of the slider, we selected three densities for simulation. They are 1.4128E3, 2.7E3, and 7.8E3kg/m<sup>3</sup>. As shown in Fig 5, the particle with the highest density moves upward sharply, while the particle with the lowest density has a much flatter trajectory. The reason is that a particle with higher density tends to move with a greater velocity relative to the air, which contributes more lift force than that experienced by a particle with lower density. Particles with low density soon reach the velocity of the air flow.

### 3.2 Multi particle flow analysis and contamination on the slider surfaces

For the multi particle flow analysis, particle sizes are chosen to have a Gaussian distribution. The mean size is 30nm, while the largest particle is 43nm, and the smallest particle has a diameter of 16nm. The particle size distribution is given in Fig. 6. Here the particle density is 2.7E3 kg/m<sup>3</sup> for all particles.

Since the gaps between the leading rail and the disk surfaces decrease from 280 nm to 100 nm along the rails in the x direction, many of the particles are blocked by the leading edge of the slider as shown in Fig. 7. Figure 7(a) shows the particle distribution in the air bearing at the initial time of the simulation, while Fig. 7(b) shows the particle distribution at T=0.18. Particles that impact and adhere to the front of the slider are no longer shown. One may see clearly that the particles are likely to contaminate the transition regions of the side rails. Also, due to the combination of lift forces and narrowing transition regions on the rails, some particles are lifted to impact these transition regions. For those particles that enter the recessed region between the

front rails, the lift forces acting on them are relatively small since the particle sizes are smaller than 100nm. The particles that contaminate the trailing rail are mainly due to the decreasing gap between the rail and disk surface. The final particle contamination profile on the slider surface is shown in Fig.8.

Figure 9 shows the comparison of particle contamination profiles for particles with different densities. The particle density in Fig. 9(a) is  $1.0E3 \text{ kg/m}^3$ , while in Fig. 9(b) it is  $7.8E3 \text{ kg/m}^3$ . More particles collected on the trailing rail of the slider for the higher density, because particles with higher density tend to move with a higher relative velocity, which contributes to larger lift forces.

To study the effect of the slider's flying characteristics on particle contamination, we considered two new designs obtained by modifying the leading pad and trailing rail. Both sliders fly at a flying height around 21 nm. But the first slider has a pitch angle of  $66.9 \mu\text{rad}$  and a roll of  $5.5 \mu\text{rad}$  and the second slider has a pitch angle of  $84.9 \mu\text{rad}$  and a roll angle of  $-5 \mu\text{rad}$ . Figure 10 shows the comparison of particle contamination on those two sliders. It is observed that very few particles contaminate the trailing rail surface of the low pitch angle slider, only one out of 500 particles contaminates on the trailing pad, as shown in Fig. 10(a). For the slider with a pitch angle of  $84.9 \mu\text{rad}$  in Fig. 10(b), 13 out of 500 particles are deposited on the trailing pad. It is also observed that more particles are blocked by the leading edge of the slider whose pitch angle is  $66.9 \mu\text{rad}$  than for the higher pitch angle slider.

#### **4 Conclusions**

From multi particle flow analysis in the air bearing we observe that many particles will deposit on the leading region of a slider due to the decreasing gap between the slider and the disk surfaces. Also, the particles are likely to contaminate

the transition regions of the rail surfaces. Larger particles are more rapidly lifted to the slider surfaces because the lift forces acting on them are larger. The density also affects the particle's flying path. The particles with higher density tend to move with a relatively high velocity in the air bearing, which contributes to the particle's contamination of the slider surface. Also, the pitch angle of a slider strongly affects the particle contamination of the slider. Lower pitch angles are desirable for controlling particle contamination on slider surfaces.

### **Acknowledgements**

This project is funded by CML, Department of Mechanical Engineering at University of California, Berkeley. The authors acknowledge the discussions with Dr. Jose Castillo, Dr. Dave Hall and Dr. D. J. Orr at Iomega Inc., Utah.

### **Nomenclature**

$Kn_d, Kn_h$	Knudsen numbers
$P$	non-dimensional pressure
$P_0$	ambient pressure
$Q$	flow factor
$R$	gas constant
$T_w, T_\infty$	temperatures
$X, Y, Z$	non-dimensional x, y, z coordinates
$U, V, W$	non-dimensional velocity components in x, y and z directions
$\bar{U}, \Delta U$	relative velocities between particle and air flow.
$\hat{U}$	normalized relative velocity between particle and air flow
$U_g, V_g$	non-dimensional velocity components in x and y directions of the air

$U_p, V_p$	non-dimensional velocity components in x and y directions of a particle
$\hat{U}$	Disk velocity
$d, D$	diameter of particle
$h_m$	nominal flying height of slider
$l$	length of slider
$m_p$	mass of particle
$t, T$	time and dimensionless time
$x, v$	particle's position and velocity vector
$\rho_g, \rho_p$	densities of gas and particle
$\sigma$	squeeze number
$\Lambda_x, \Lambda_y$	bearing numbers
$\omega_{px}, \omega_{py}$	angular velocities of a particle
$\Omega_x, \Omega_y$	normalized angular velocities of the particle

## References

- [1] Burgdorder, A., 1959, "The Influence of the Molecular Mean Free Path on the Performance of Hydrodynamics Gas Lubricated Bearing", ASME Journal of Basic Engineering, **81**(1), pp.94-100.
- [2] Cha, E. T. and Bogoy, D. B., 1995, "A Numerical Scheme for Static and Dynamic Simulation of Sub ambient Pressure Shaped Rail Sliders", ASME Journal of Tribology, **117**, pp.36-46.
- [3] Chen, X., 1996, "The Drag Force acting on a Spherical Non-evaporating or evaporating particle immersed into a rarefied plasma flow", Journal of Physics D: Applied Physics, **29**, pp. 995-1005.
- [4] Clift, R. Grace, J. R. and Weber, M. E., 1978, Bubbles, Drops, and Particles, Academic Press.
- [5] Fukui, S. and Kaneko, R., 1988, "Analysis of Ultra-thin Gas Film Lubrication Based on Linearized Boltzmann Equation: First report-Derivation of a Generalized Lubrication Equation Including Thermal Creep Flow", ASME Journal of Tribology, **110**, pp.253-261.
- [6] Fukui, S. and Kaneko, R., 1990, "A Database for Interpolation of Poiseuille Flow Rates for High Knudsen Number Lubrication Problems", ASME Journal of Tribology, **112**, pp. 78-83.
- [7] Hsia, Y. T., Domoto, G. A., 1983, "An Experimental Investigation of Molecular Rarefaction Effects in Gas Lubricated Bearings at Ultra -low Clearance", ASME Journal of Tribology, **105**(1), pp. 120-130.
- [8] Liu, V. C., Pang, S. C. and Jew, H., 1965, "Sphere Grad in Flows of Almost -Free Molecules", Physics of Fluids, **8**(5), pp. 788-796.

- [9] Lu, S. and Bogy, D. B., 1994, "A Multi-Grid Control Volume Method for the Simulation of Arbitrarily Shaped Slider Air Bearing with Multiple Recess levels", CML Technical Report, No. 94-016, Department of Mechanical Engineering, University of California at Berkeley.
- [10] Maxey, M. R., 1993, "The Equation of Motion for a Small Rigid Sphere in a Nonuniform or Unsteady Flow", *Gas-Solid Flows*, ASME FED **166**, pp. 57-62.
- [11] McLaughlin, J. B., 1993, "The Lift on a Small Sphere in Wall-bounded Linear Shear Flows", *Journal of Fluid Mechanics*, **246**, pp. 249-265.
- [12] Millikan, R. A., 1923, "The General Law of Fall of a Small Spherical Body through a Gas, and Its Bearing Upon the Nature of Molecular Reflection from Surfaces", *Physics Review*, **22**(1), pp. 1-23.
- [13] Rubinov, S. I. and Keller, J. B., 1961, "The Transverse Force on a Sphere Moving in a Viscous Fluid", *Journal of Fluid Mechanics*, **11** (3), pp. 447-459.
- [14] Saffman, P. G., 1965, "The lift on a Small Sphere in a Slow Shear Flow", *Journal of Fluid Mechanics*, **22**, pp. 385-400.
- [15] Schaaf, A. L. and Chambre, P. L., 1961, *Flow of Rarefied Gases*, Princeton University Press, Princeton, US.
- [16] Zhang, S., 1997, *Numerical Investigation of Particle Contamination and Thermal Effects in a Slider Disk Interface*, Doctoral Dissertation, Department of Mechanical Engineering, University of California, Berkeley.
- [17] Zhang, S. and Bogy, D. B., 1996, "Effects of Lift on the Motion of Particles in the Recessed Regions of a Slider", CML Technical Report, No. 96-016, Department of Mechanical Engineering, University of California at Berkeley.



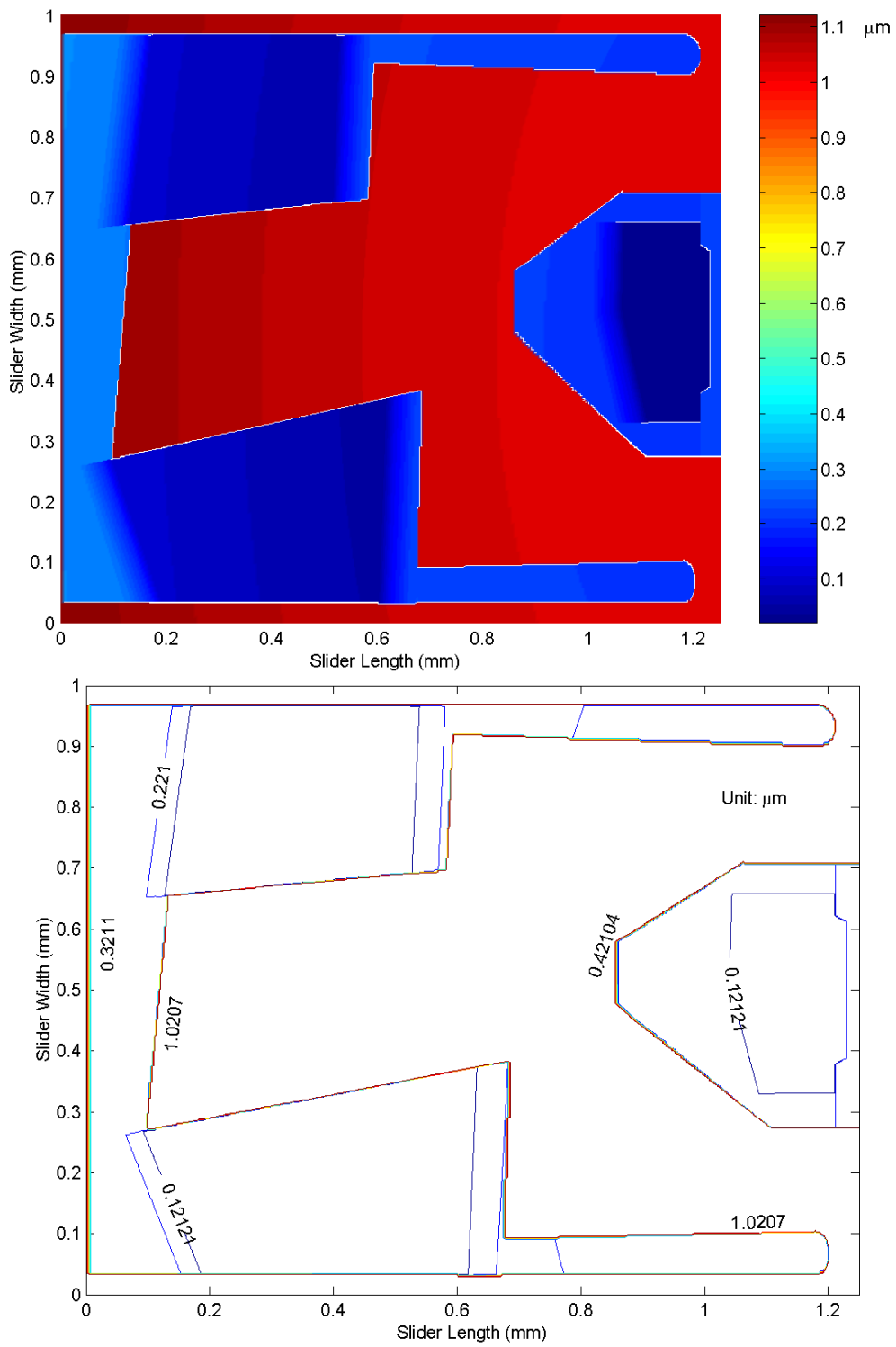


Fig. 3 Flying height Contour of the slider

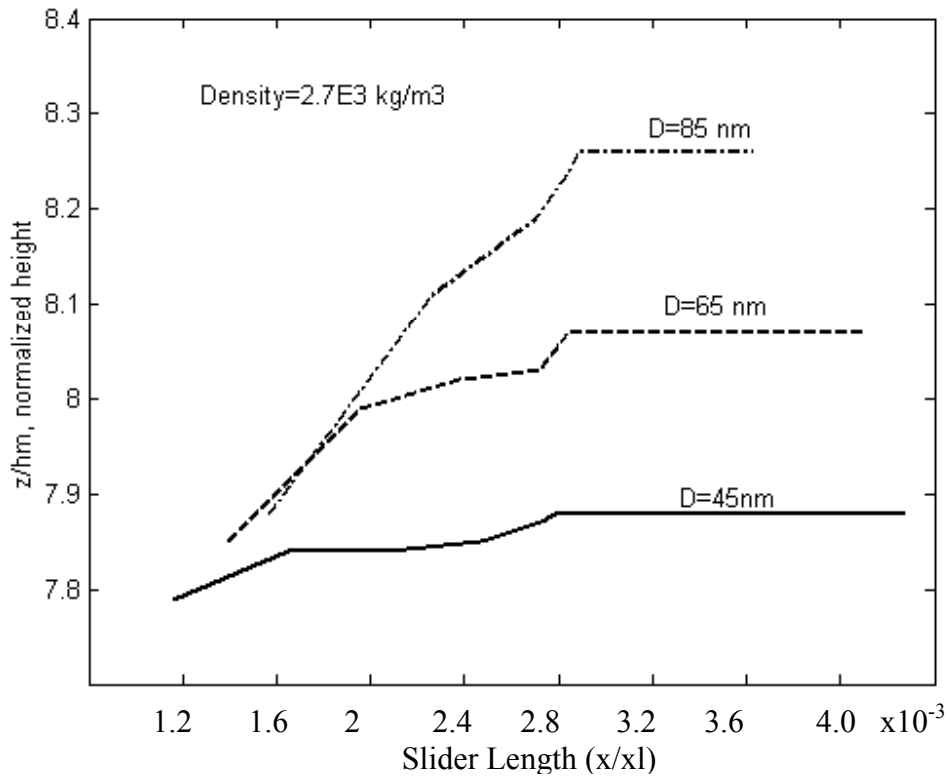


Fig. 4 Effects of particle sizes on its flying path in the air bearing

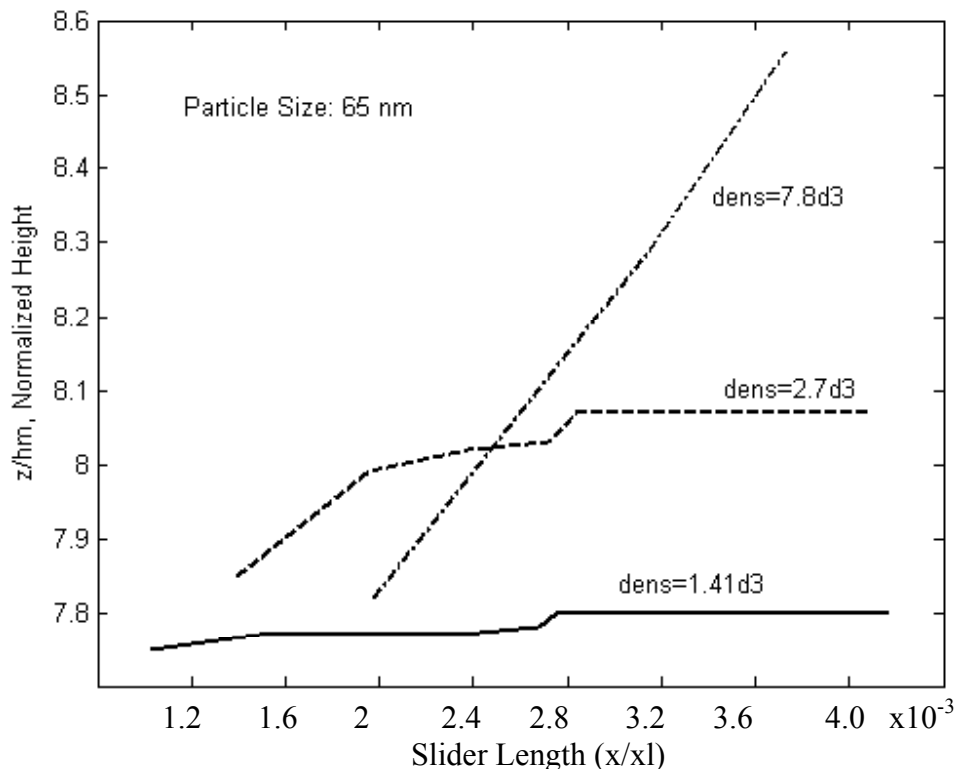


Fig. 5 Effects of density on particle's flying path in the air bearing

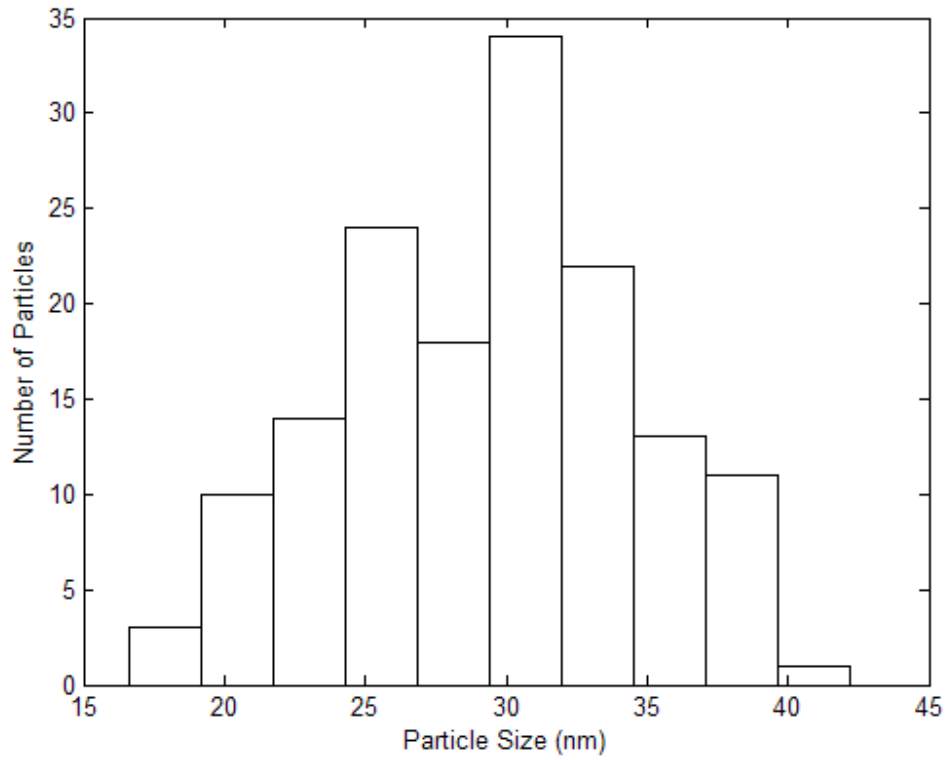


Fig. 6 Particle sizes of Gaussian distribution, mean size=30nm.

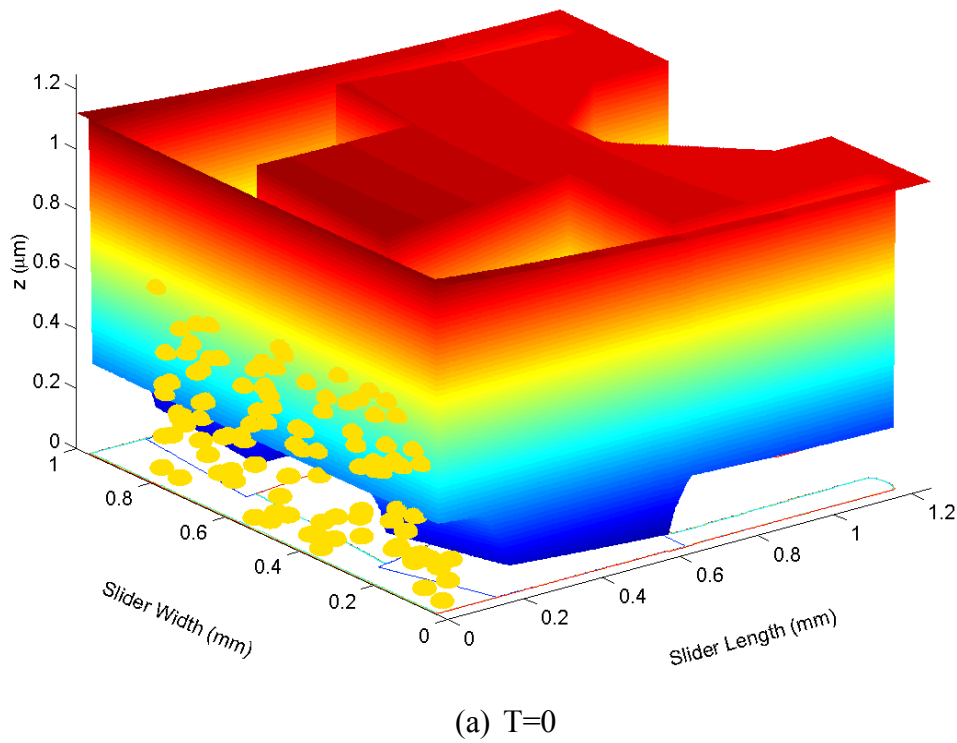
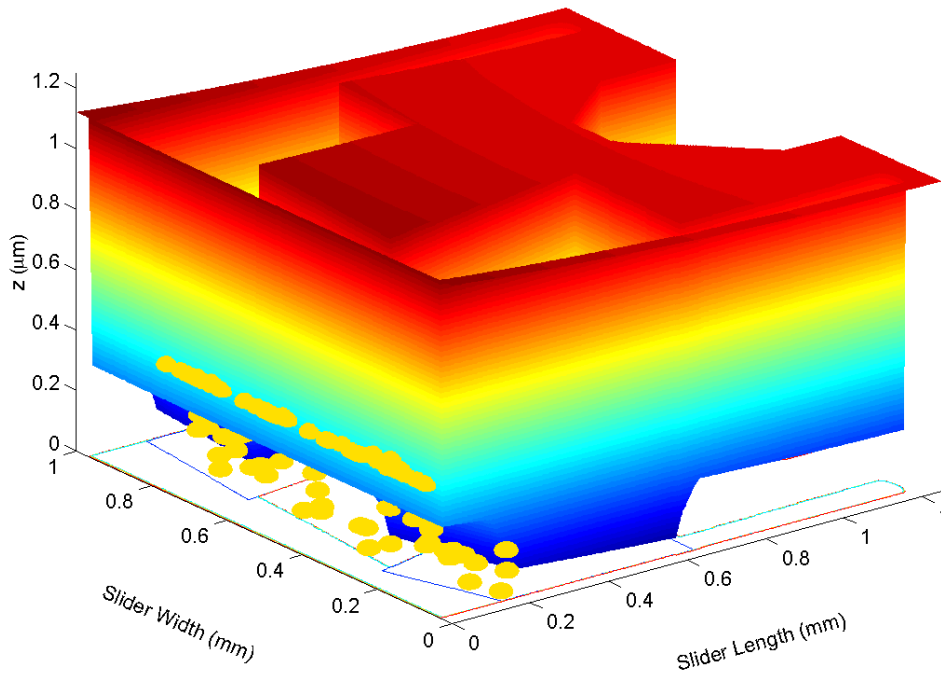


Fig. 7(a) Time-dependent 3-D particle distributions in the air bearing



(b)  $T=0.18$

Fig. 7(b) Time-dependent 3-D particle distributions in the air bearing

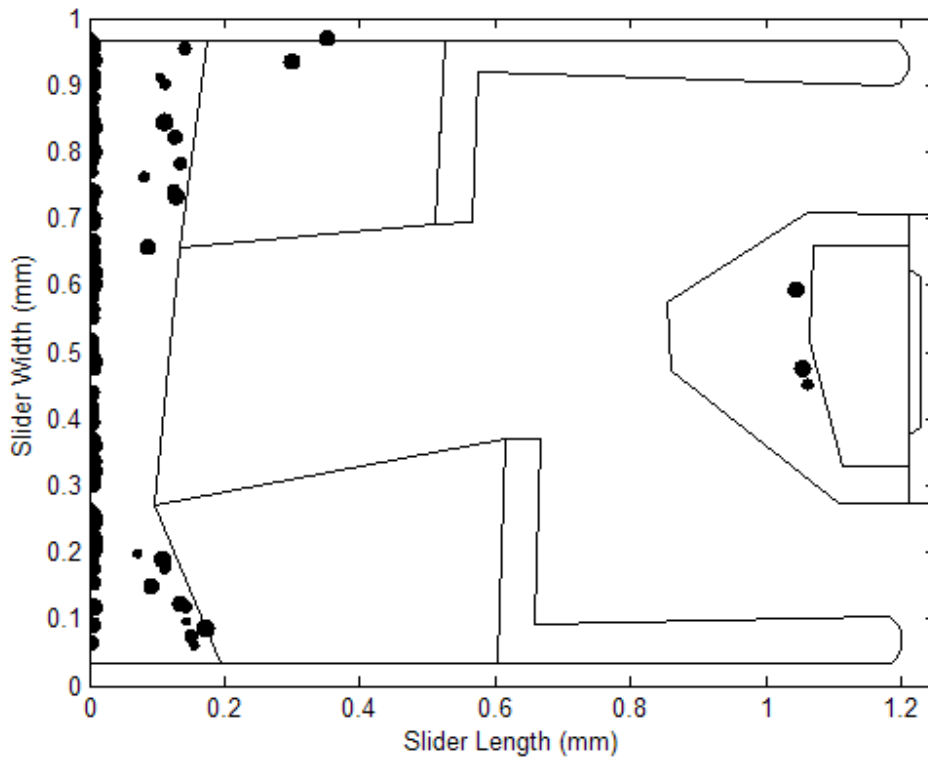
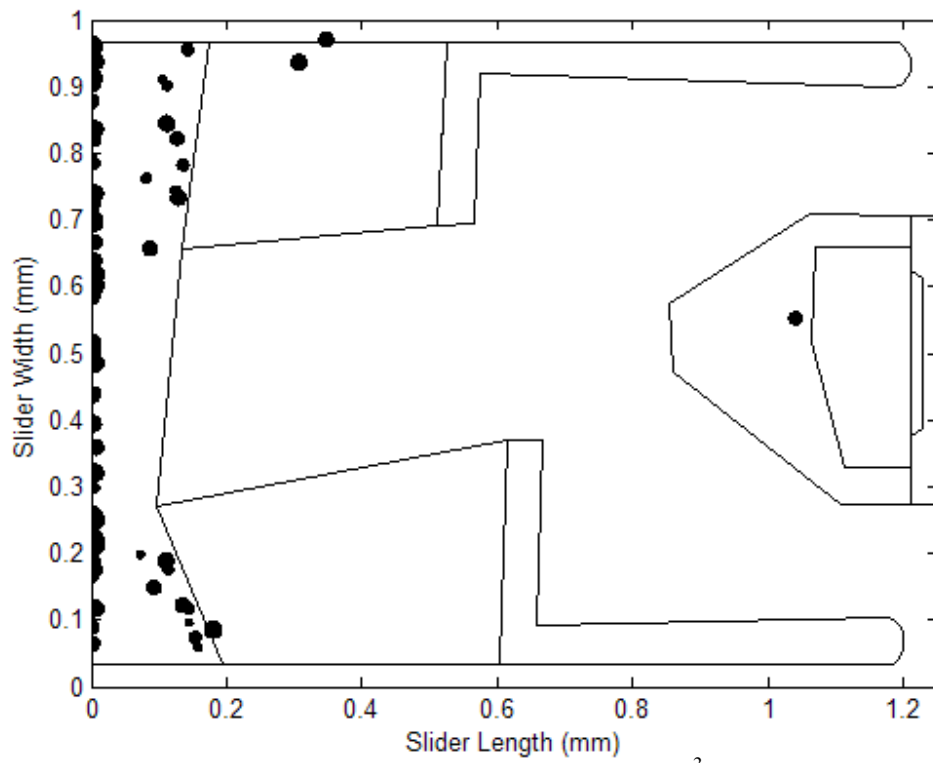
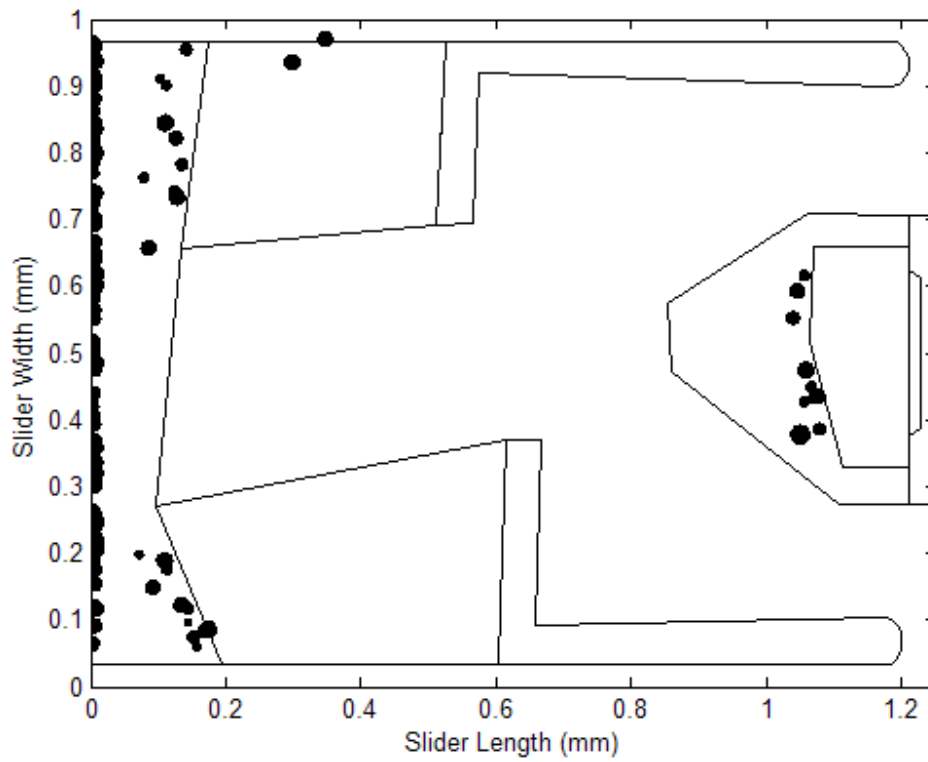


Fig. 8 Particle contamination profile on one slider surface

(FH=25.6 nm, Pitch=75  $\mu\text{rad}$ , Roll=-1.79  $\mu\text{rad}$ )

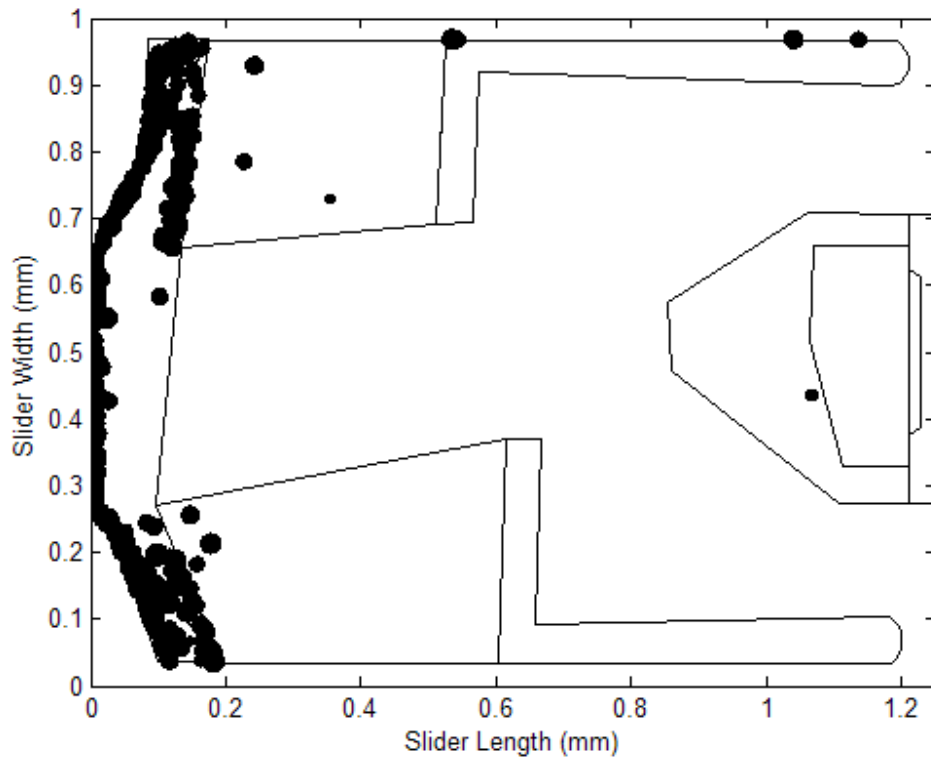


(a) Density=1.0E3 kg/m<sup>3</sup>

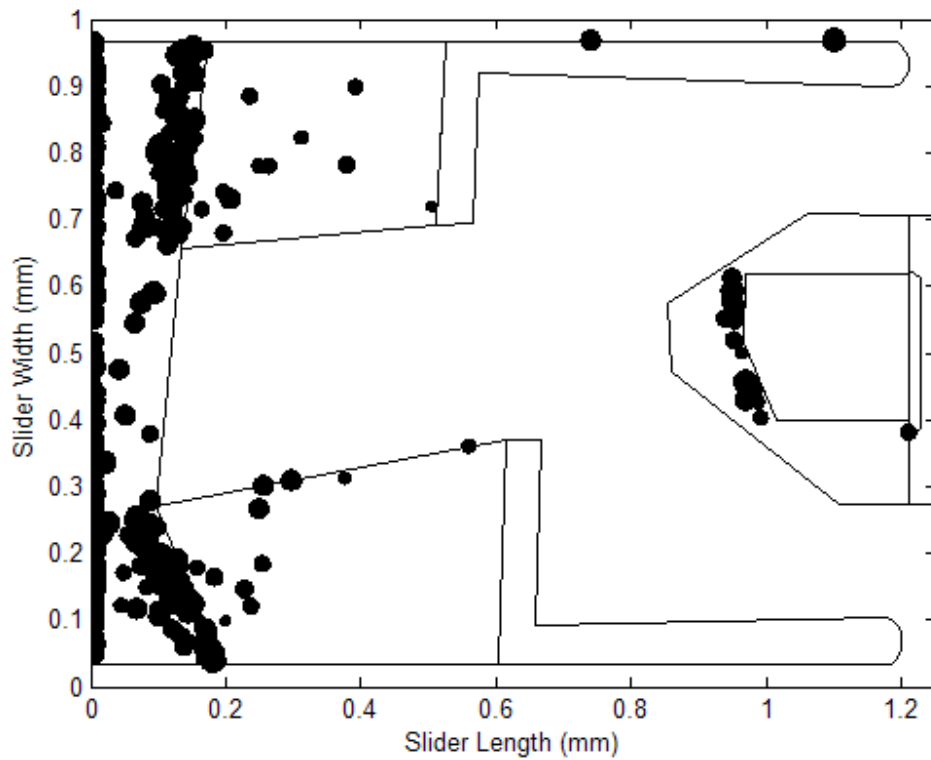


(b) Density= 7.8E3 kg/m<sup>3</sup>

Fig. 9 Effect of particle's density on particle contamination behavior on slider surfaces



(a) FH=21.5 nm, Pitch=66.9  $\mu$ rad, Roll=5.5  $\mu$ rad



(b) FH=20.1 nm, Pitch=84.9  $\mu$ rad, Roll=-5  $\mu$ rad

Fig. 10 Effect of pitch angles on particle contamination behavior on slider surfaces